

Note SEM Applications

MATERIALS LABORATORY		
HEB	TEB	SEC
HEB	TEB	SEC
RCE	ROH	WED
Ref. CEW	DEW	WDE
DJW	TBS	REM
JAC	JLW	JLJ
FILE		



SOCIETY OF AUTOMOTIVE ENGINEERS, INC.
Two Pennsylvania Plaza, New York, N.Y. 10001

Failure Analysis of a Shot-Peened Component

Om Johari
ITT Research Institute

William A. Sipes
Naval Air Development Center

SOCIETY OF AUTOMOTIVE ENGINEERS

Automobile Engineering Meeting
Detroit, Mich.
May 14-18, 1973

730579

ABSTRACT _____

A comprehensive scanning electron microscope (SEM) survey of the fracture surfaces of an aircraft main landing gear shock strut piston showed that improper shot peening contributed to the initiation of the anomalous fatigue failure.

SEM photographs of the suspect-origin regions and the surrounding areas were analyzed. The photographs are presented, along with a detailed description of the regions observed. Failure mechanism is discussed, and causes of fracture origin explored. _____

Failure Analysis of a Shot-Peened Component

Om Johari

ITT Research Institute

William A. Sipes

Naval Air Development Center

THIS PAPER PRESENTS an analysis of an aluminum shock strut piston failure in a naval aircraft*. The part was obtained from the Naval Air Development Center (NADC), Johnsville, Pa., where it had been forwarded from the Naval Air Rework Facility at Norfolk, Va. The material was identified as 7075 aluminum alloy, heat-treated to the T6 condition. The hardness of the failed part was Rockwell B-80.

Before receipt of the sample at IIT Research Institute (IITRI), it had been analyzed by the NADC using optical and replica transmission electron fractography (1)**. Fig. 1 shows the overall fracture surface, Fig. 2 the elevation view of the failed piston (1), and Fig. 3 an overall view of the part as received by IITRI. We did not have access to the other half of the fracture. Close-ups of areas 1 and 3, as shown in Figs. 4 and 5, were examined in detail. A cursory examination of areas 2 and 4 indicated them to be identical to 1 and 3. The identification of fracture mode was not possible from optical macrofractographs alone. The information provided by NADC indicated it to be a fatigue failure (1).

EXPERIMENTAL METHOD

Specimens of interest were cut from the as-received part (Fig. 3). These specimens were cleaned ultrasonically in trichloroethylene, although some parts did not clean up even after repeated ultrasonic immersions. The specimens were examined in a JSM-2 scanning electron microscope (SEM)

*The opinions expressed are the private ones of the authors and are not to be construed as official or reflective of the views of the Department of the Navy or the authors' respective organizations.

**Number in parentheses designates Reference at end of paper.

at a range of magnifications. Many of the photographs were taken as stereopairs.

RESULTS

The results are presented in two parts: the first deals with examination of the suspect-origin regions, the second with the surrounding areas.

SUSPECT-ORIGIN REGIONS - Fig. 6 presents a composite photograph of area 3, while Fig. 7 is a higher magnification

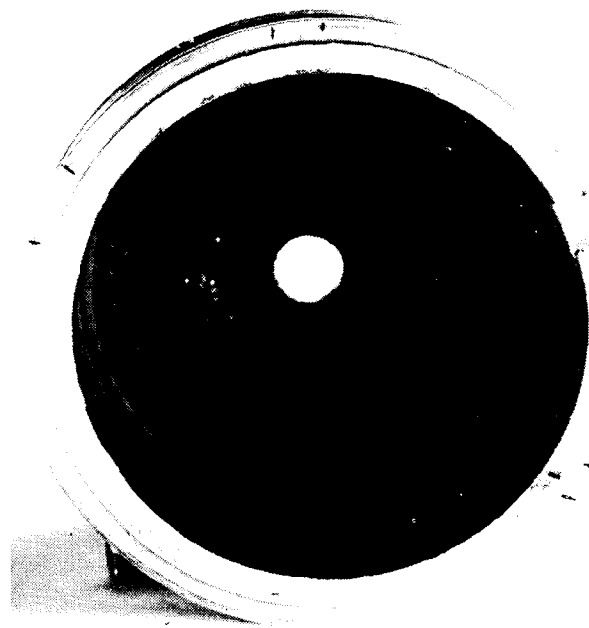


Fig. 1 - Plan view of failed piston in as-received condition by Naval Air Development Center



Fig. 2 - Elevation view of failed piston in as-received condition by Naval Air Development Center

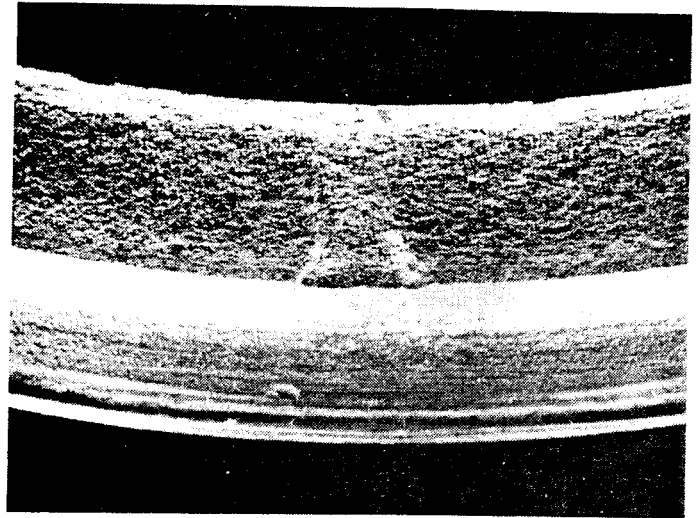


Fig. 4 - Close-up of area 1 in Fig. 3. Magnification 5X

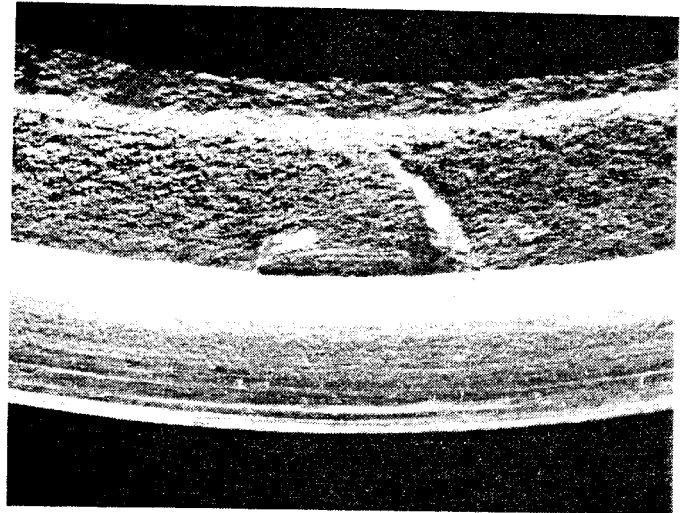


Fig. 5 - Close-up of area 3 in Fig. 3. Magnification 5X

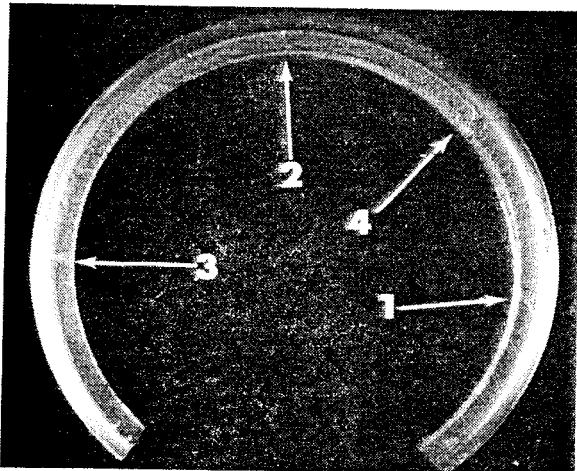


Fig. 3 - Failed part in as-received condition by IITRI indicating areas examined



Fig. 6 - Composite of four SEM photographs showing suspect-origin region. Shot-peened surface is on right side. Stereo examination revealed that crescent-shaped region SS was at lower plane than rest of fracture face. Failure was suspected to have originated at center of SS. Magnification 27X reduced 78% for reproduction

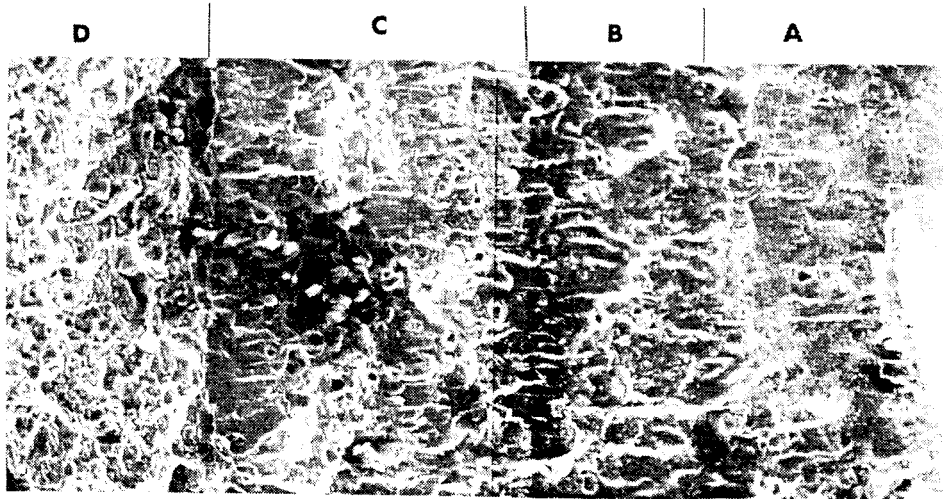


Fig. 7 - Region at center of SS in Fig. 6. showing four distinct regions A, B, C, and D. Magnification 140X reduced 77% for reproduction

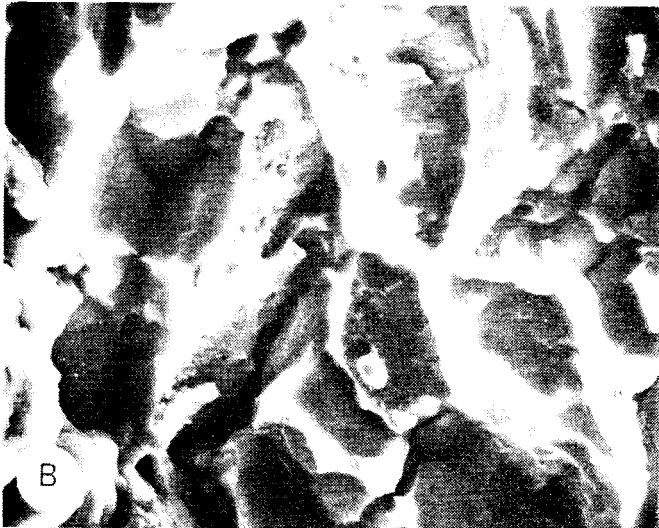
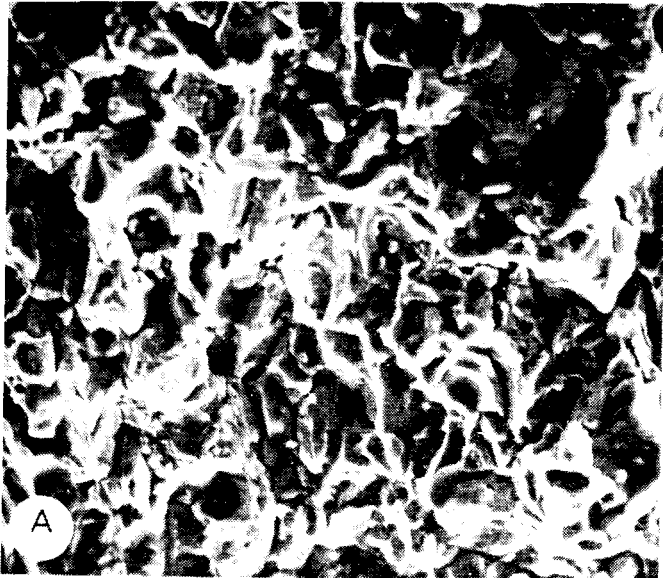


Fig. 8 - Typical features of region D in Fig. 7 showing overload failure. Magnification: A - 300X, B - 1000X

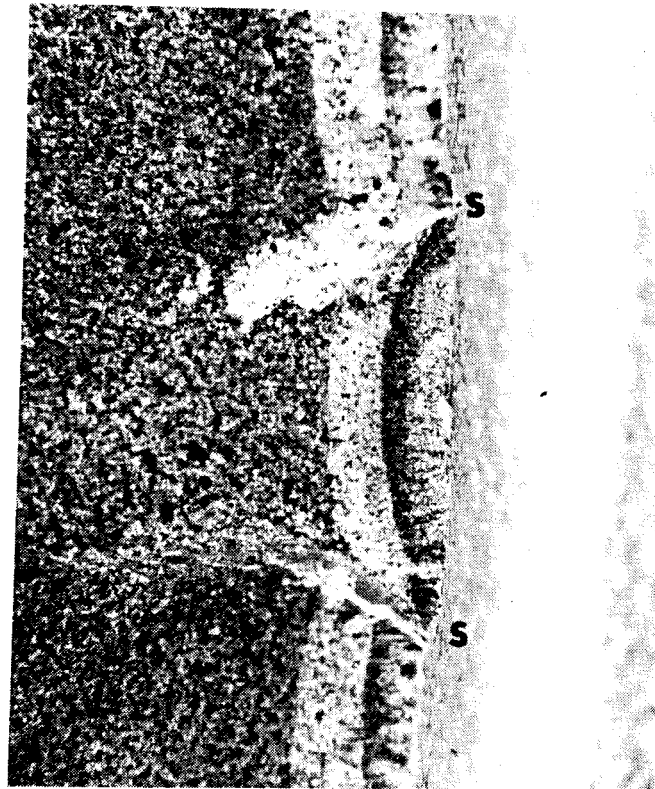


Fig. 9 - Optical macrophotograph of suspect origin in specimen 3. Magnification 18X

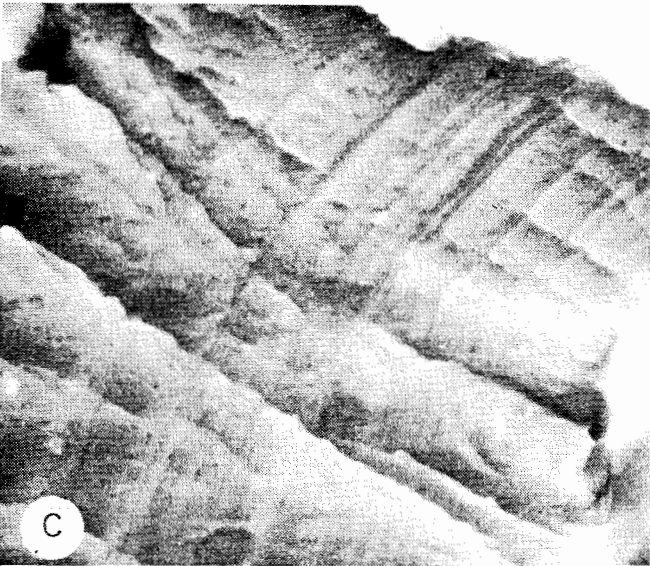
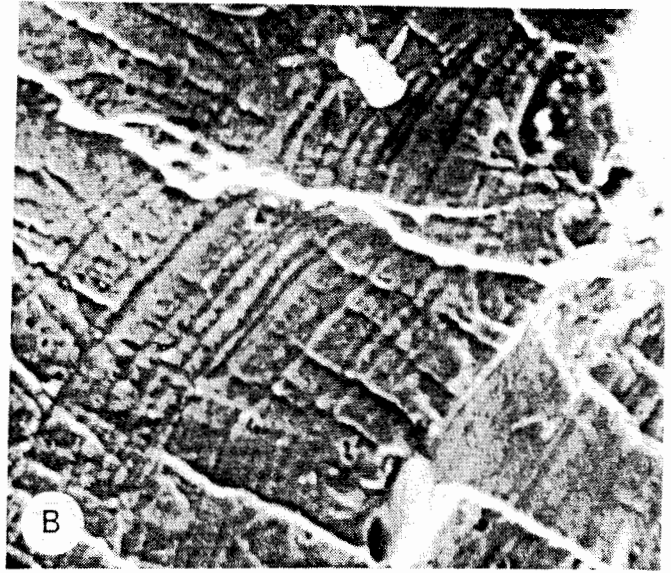
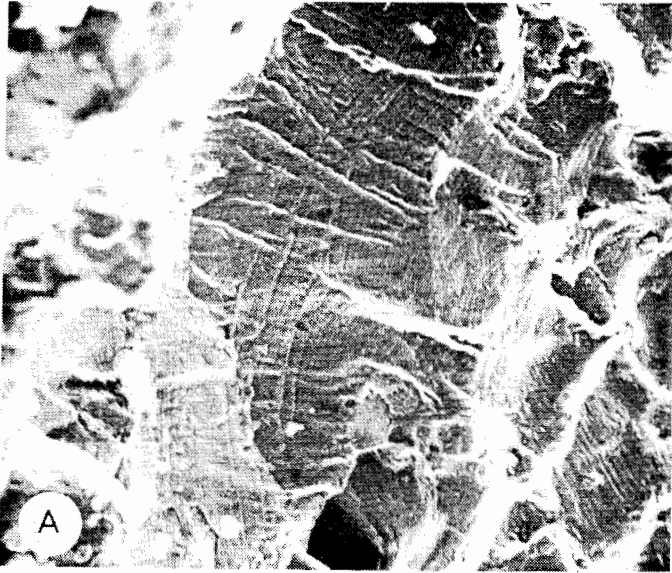


Fig. 10 - Fatigue striations in region C. A—low magnification, 810X. While most striations point to center of SS as origin, local differences in striation directions, attributed to individual grain orientation, are also seen. B—higher magnification (2700X) of top central region in Fig. 10A. C—another region showing striations in regions C. SEM was operated at 25 kV for this photograph, and at 5 kV for photographs in Figs. 10A and B, thus accounting for different appearance. Magnification 3000X

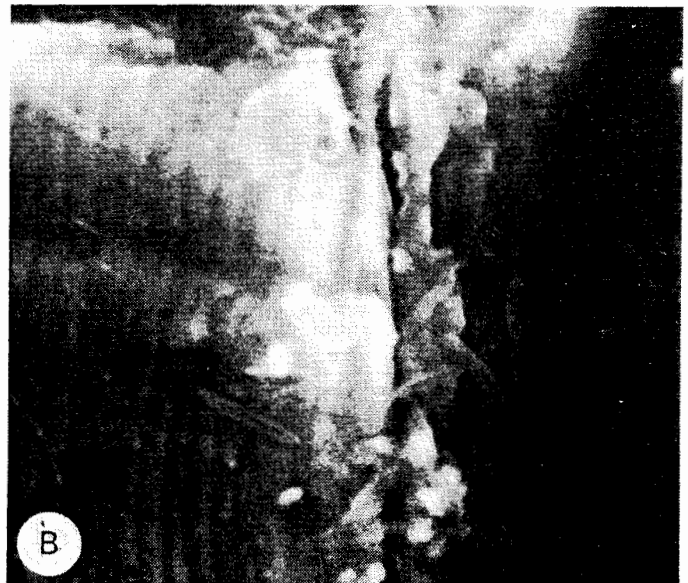


Fig. 11 - Region C on left and region B on right. Demarcation between two regions is clearly observed. Magnification: A—500X, B—6000X

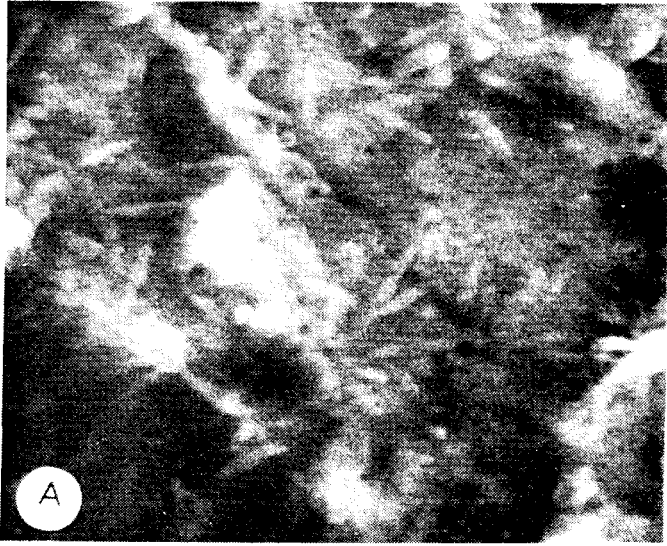


Fig. 12 - Details of contaminants covering most of region B. Magnification 7700X

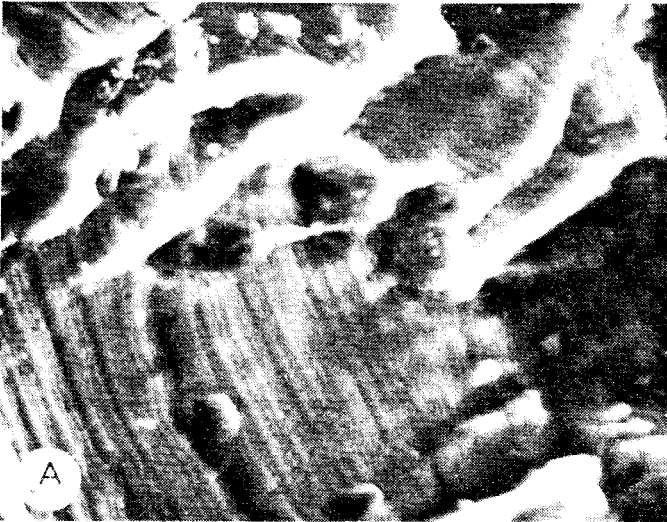


Fig. 13 - Fatigue striations in (A) region C (magnification 2300X) and (B) region B (magnification 2300X). Striations are clearer and sharper in region C than in region B, where they are obscured by contaminants

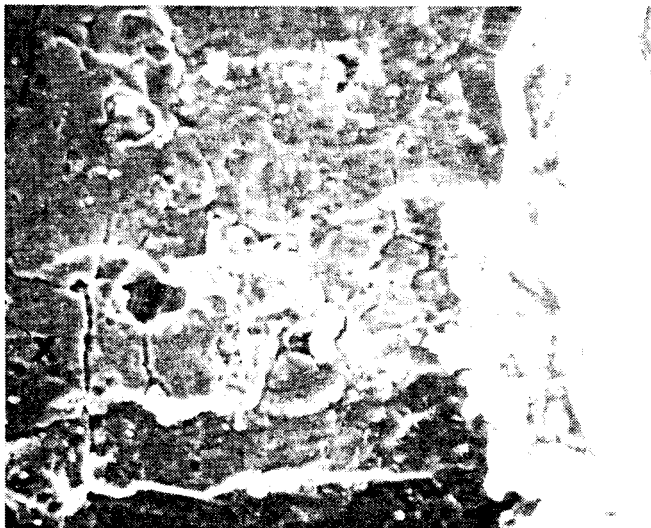
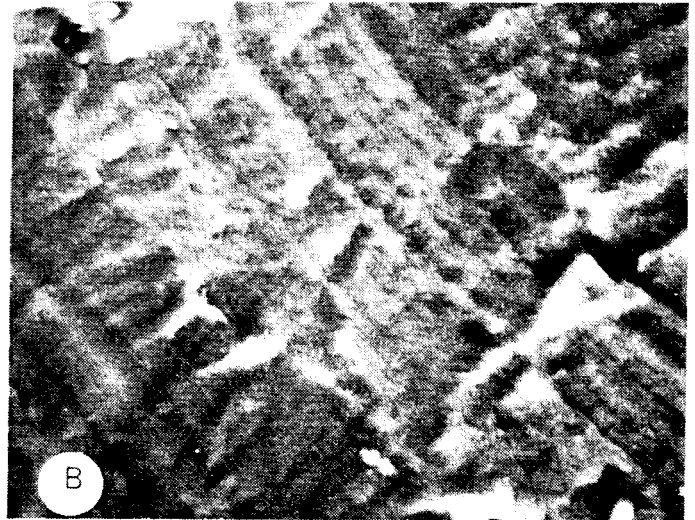


Fig. 14 - High magnification view of region A at center of fracture edge in Fig. 7 magnification: 460X

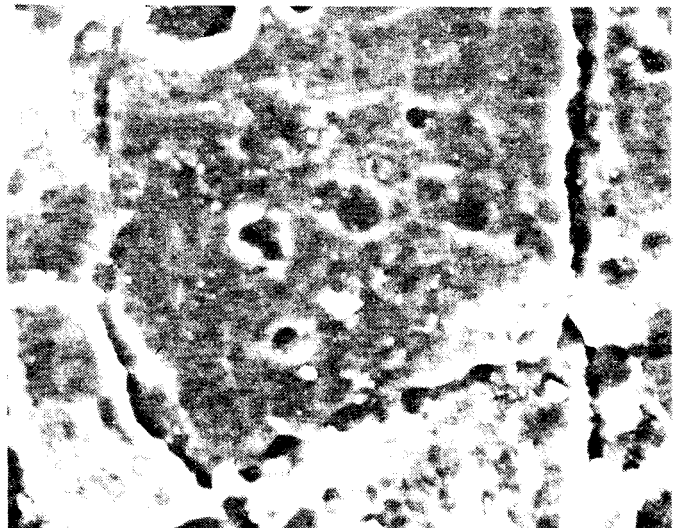


Fig. 15 - Details of grain X in Fig. 14, showing pitting and grain boundary attack. Magnification: 1380X

view of the center of region SS of Fig. 6. Four distinct regions are identified, A, B, C, and D. A being closest to the outside shot-peened surface, D being the final fracture overload region. Typical features of region D are illustrated in Figs. 8A and 8B. Regions B and C were clearly separated because, both in high-magnification optical macrofractographs (Fig. 9) and in SEM photographs, region B was much darker than region C. Typical fatigue striations could be readily observed in region C. The direction of striations pointed toward the center of area SS as the origin, though local effects of grain orientations were also observed (Figs. 10A-10C). Except toward the edges of crescent SS (as shown in Fig. 10), the striations, for the most part, were parallel to the circumference of the ring-shaped sample.

Figs. 11A and 11B show that the boundary between regions B and C is clearly separated. In general, region B was heavily contaminated; the film which was present could not be removed by repeated ultrasonic cleaning. The structure of

the contaminants is clearly brought out at high magnification in Fig. 12. Fig. 13 presents a comparison between regions B and C. The fatigue features can be seen at some locations in region B, but at most locations the features are totally obscured due to being covered by the contaminants.

In region A, no specific initiation point could be found; Fig. 14 is a high-magnification photograph of this region. Grain boundaries were separated and were clearly identified in most areas of region A. The structure here appears to have been induced by chemical attack (Fig. 15).

AREAS AROUND SUSPECT-ORIGIN REGION - In the

area outside the suspect-origin region described (that is, outside region SS of Fig. 6), four similar regions were observed (Figs. 16A and 16B). The features of regions C and D were identical. In all areas of regions B and C the striations were parallel to the circumference of the sample (Figs. 17 and 18). The darker region B (Figs. 17A and 17B) was again more contaminated than region C, and though fatigue features are suspected, they could not be clearly resolved. In Figs. 18A-18C the boundary between B and C is, again, very distinct. Area A (Figs. 19A and 19B) is also very similar in the regions inside and outside SS of Fig. 6.

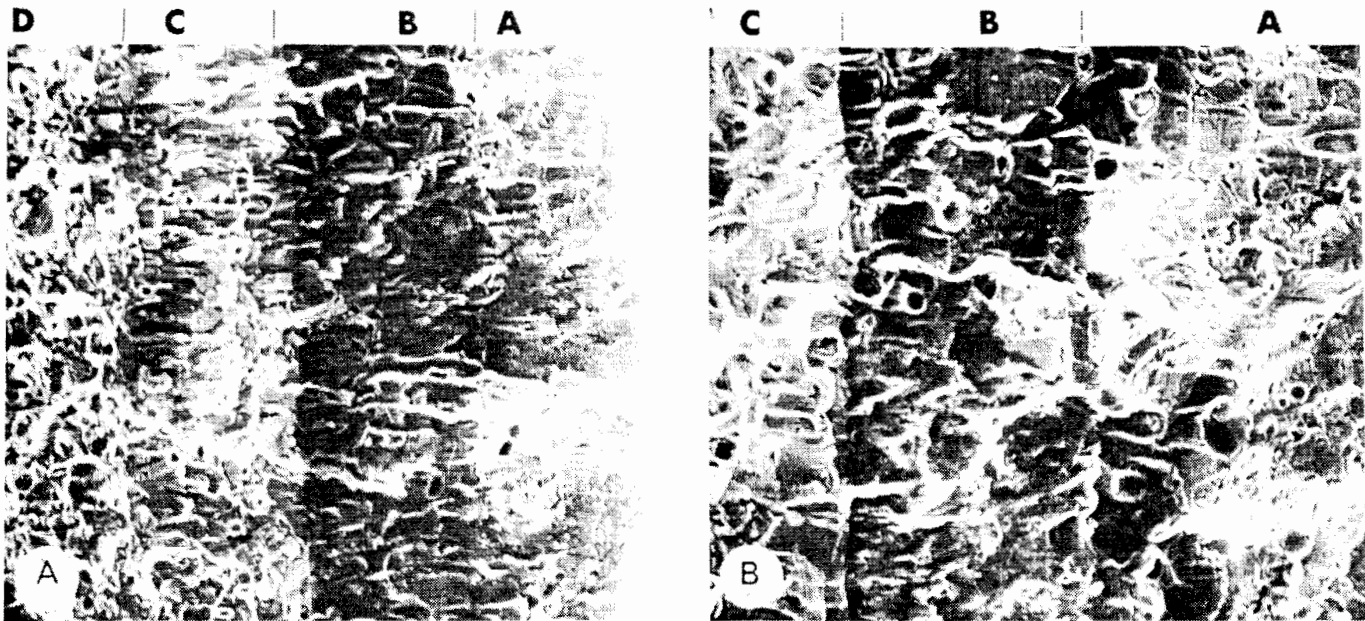


Fig. 16 - Two areas outside crescent-shaped suspect-origin SS. Four regions (A, B, C, and D), identical to Fig. 7 are observed. Magnification: A-100X, B-230X

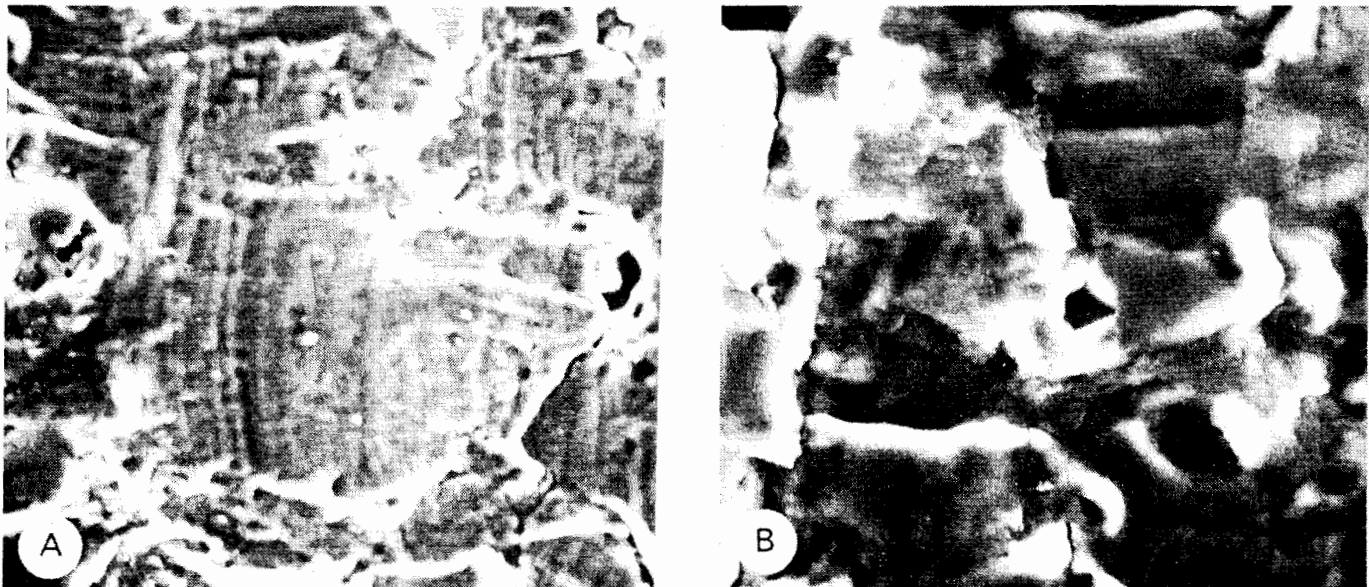


Fig. 17 - Two views of region B. In (A) presence of fatigue striations is not as clear as in left sides of Fig. 18, and in (B) fatigue features are not resolved due to surface contaminants. Magnification: A-770X, B-1000X

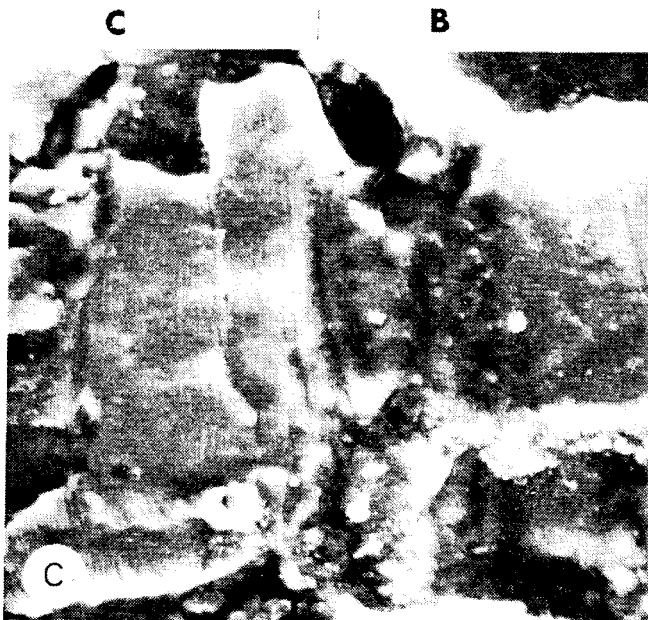
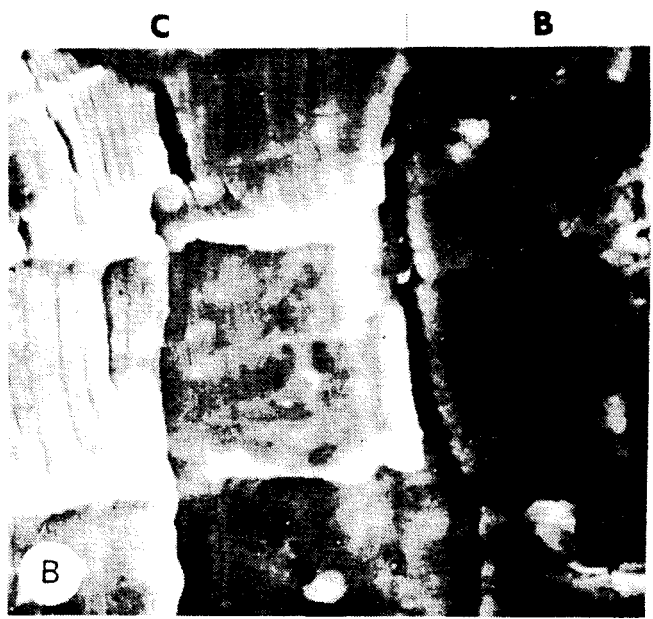


Fig. 18 - Views of regions B and C. A--region B on right and region C on left (500X). B--high magnification (2300X) view of center of Fig. 18A, showing striations in region C and contaminants in region B. C--another area (1000X) showing identical features in regions B and C as in Fig. 18B

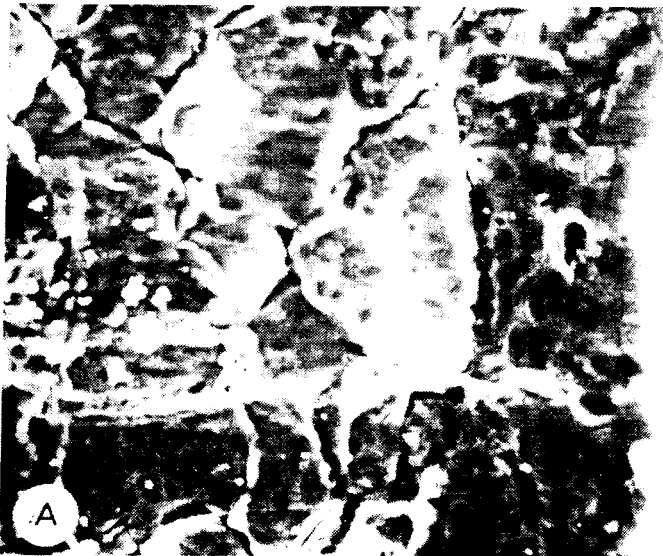


Fig. 19 - Appearance of region A outside crescent region SS. Features are similar to those of region A in Figs. 14 and 15. Magnification: A--770X, B- 2300X

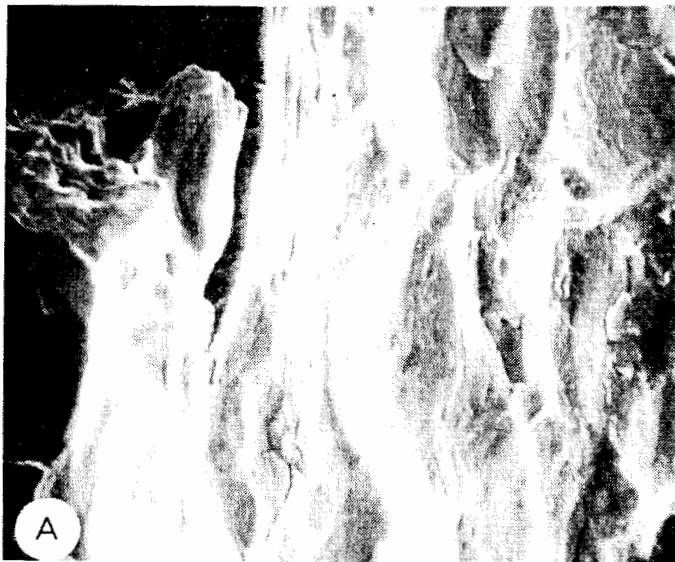


Fig. 20 - Study of shot-peened surface. A—crack on shot-peened surface at lower end of crescent region SS. B and C—many areas on shot-peened surface showed presence of original machine markings. Some areas were either unexposed or lightly exposed to shots, due to poor shot-peening control, and hence resulted in local regions of high tensile stresses. Magnification: A—180X, B—180X, C—500X

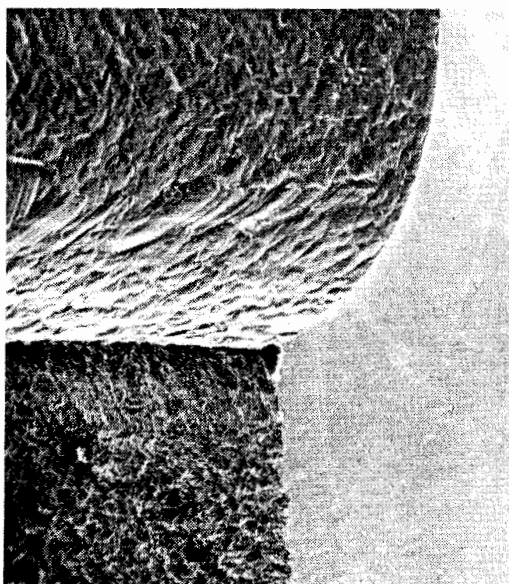


Fig. 21 - SEM enables examination of all three surfaces at one time. Polished surface is on right, shot-peened surface on top left, and fracture surface on bottom left. Magnification: 24X

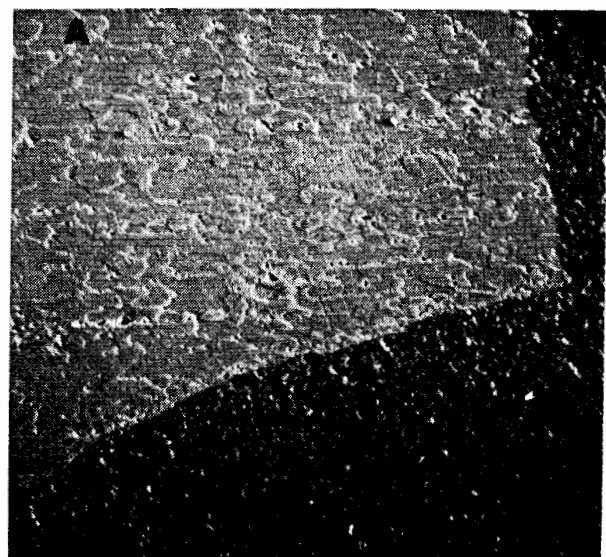


Fig. 22 - Backscattered SEM photograph. Section through shot-peened surface (curved edge) and fracture surface (straight edge) showing microstructure of alloy as revealed by SEM. Sample is mounted in bakelite. Magnification: 100X

DISCUSSION

Based on the reported results, it is established that the mechanism of failure was fatigue and the final fracture was by overload. Region C showed fatigue striations at all locations around the circumference of the fracture face more clearly than region B, although some fatigue features were also observed in region B. Since the component is a shock strut, this evidence suggests that, after the crack propagated to the end of region B, either it stopped for a considerable length of time or the strut was exposed to a hostile environment allowing contamination to build up on the opened crack. Many possible sources of this contamination, as well as the chemical attack observed at region A, could be encountered by the strut during its use on a naval aircraft. The crack propagation in regions C and D leading to final fracture

possibly occurred during a shorter period of service or was in a less hostile environment, so that this area remained relatively free of contamination.

The identical nature of A areas (Figs. 14 and 19) in SS regions (there were at least five such regions at various points on the circumference of the section received) and outside SS is attributed to continuous rubbing and smearing in this area which fractured first, and chemical attack resulting from exposure to corrosive environments during the life of the part since this area, being closest to the specimen surface, suffers maximum exposure. Also, alkaline solutions are used to clean aluminum alloy components, and the structure in Figs. 14 and 19 could arise from the use of such solutions before the crack opened beyond the initial stages of region B.

No specific cause of fracture origin could be established from the above observations. The crescent-shaped regions

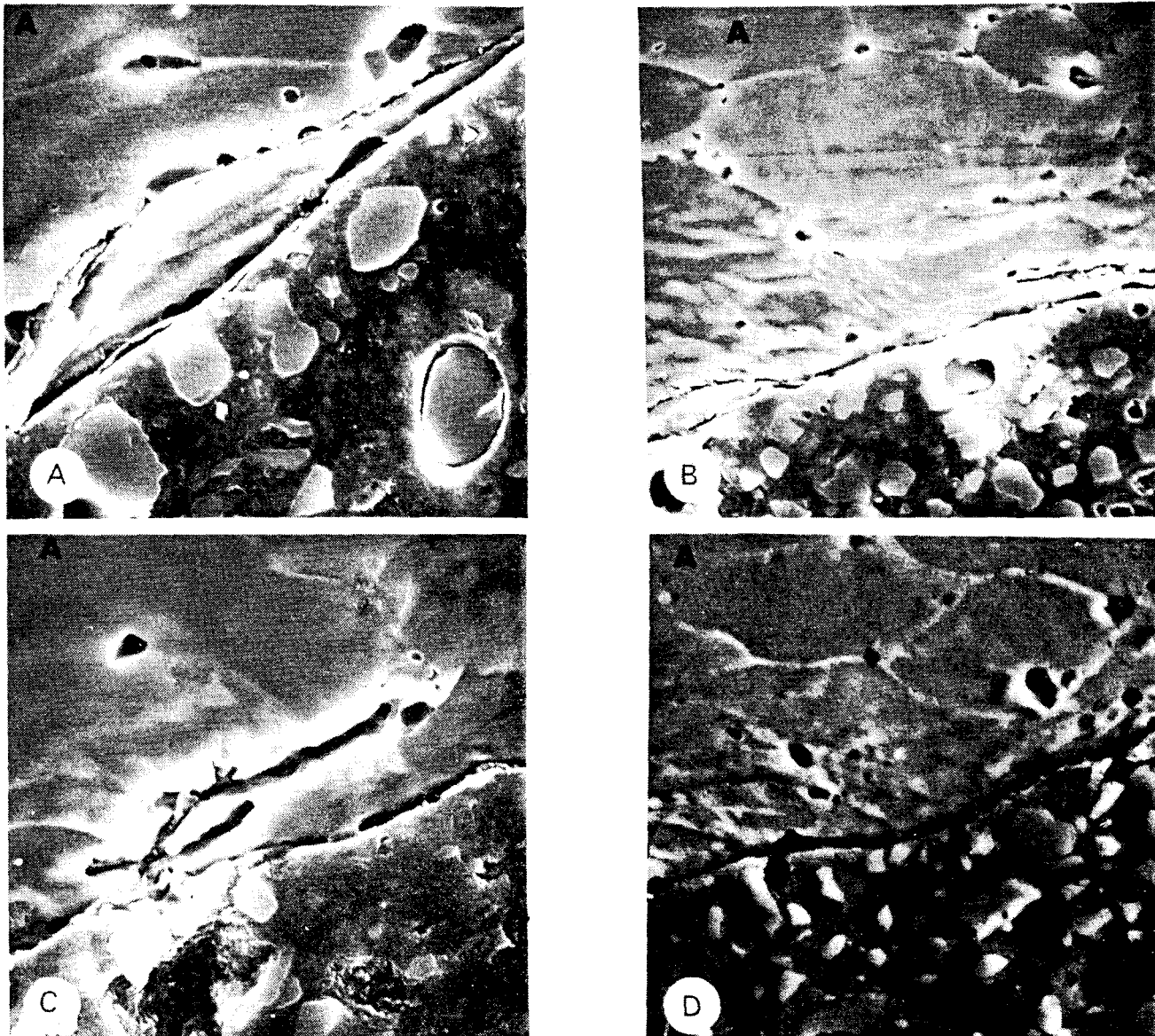


Fig. 23 - Four views showing details of shot-peened edge in Fig. 2. Notice extent of deformation induced and nature of defects which are present. (All micrographs are secondary electron images in SEM.) A—alloy, B—bakelite. Magnification: A—2000X, B—1000X, C—2000X, D—1000X

always occurred in a plane below the minimum cross-section plane containing most of the fracture. The specimen had been shot peened, and a study of the shot-peened surface revealed many defects; some areas showed surface cracks and many areas showed original machine markings suggesting improper control of shot-peening parameters (Fig. 20).

Region A in the areas observed (for example, Figs. 7 and 16) extends to approximately 0.025 cm below the shot-peened surface. Since shot peening is employed to prevent fatigue failures by providing compressive stresses at the immediate surface (usually the first 0.013 cm or less), observations such as in Fig. 20 indicate that many areas were either not hit or very lightly hit by the shots and derived no benefit from the shot-peening operations. Large isolated areas of unfavorable stress states caused by poorly controlled shot peening and located at or near the minimum section of the strut could thus act as initiation sites. The observations of many suspect initiation sites support this explanation, although precise correlation between any surface defects and fatigue initiation sites was not found.

To verify the shot peening damage further, a metallographic section was prepared (Figs. 21 and 22). Detailed SEM examination of this section (Fig. 23) revealed presence of many flaws and confirmed the uneven nature of shot-peening load distributions.

The following failure mechanism is proposed based on the above results and discussion. Sipes (1) had proposed a similar mechanism and, in that respect, our results and conclusions, based on definite experimental evidence observable only by SEM, support Sipes' hypothesis. The crack initiated at any surface defects (probably shot-peening defects, with or without machining defects) and propagated to the end of region A. The changed stress state then caused the cracks from these locations to propagate along the circumference until they met, and the entire A region was opened up exhausting any

beneficial effects of shot peening. This could have been confirmed by presence of radial striations in areas A, but except for two isolated observations, the smeared and chemically attacked condition of region A prevented such confirmation. Following this, the crack propagated by fatigue during each loading cycle, opening up more and more of the specimen cross section (through regions B and C) until a critical cross section was reached, at which time the strut was no longer able to support the load and final fracture occurred by overload.

CONCLUSIONS

1. Fractographic analysis showed that failure was by a fatigue mode initiated at many points at the base of a peripherally machined groove acting as a notch in the narrowest cross section of the failed part.
2. Improperly applied and controlled shot peening contributed to the initiation of failure in that it provided sites of microcracking in the plane of stress determined by the machined groove.

ACKNOWLEDGMENT

The samples were provided by the Naval Air Rework Facility, Norfolk, Va., through the Analytical Rework Program of the Naval Air Systems Command (AIR-4117). This work was performed under NASA Contract No. NAS1-10788, and was submitted as NASA Contractor Report NASA CR-2166 dated January 1973.

REFERENCE

1. W. A. Sipes, Naval Air Development Center, Report No. NADC-MA-7061, October 1970 (AD 875653L).